Biosensors and Bioelectronics 129 (2019) 292–297

Contents lists available at ScienceDirect

Biosensors and Bioelectronics

journal homepage: www.elsevier.com/locate/bios

Measuring fluorescence-lifetime and bio-impedance sensors for cell based assays using a network analyzer integrated circuit

Markus Hefele[a,*], Walter Wirths[b], Martin Brischwein[c], Helmut Grothe[a], Franz Kreupl[a], Bernhard Wolf[b,d]

[a] Technical University of Munich (TUM), Department of Hybrid Electronic Systems, Arcisstr. 21, 80333 Munich, Germany
[b] Technical University of Munich (TUM), Department of Electrical and Computer Engineering, Arcisstr. 21, 80333 Munich, Germany
[c] Technical University of Munich (TUM), Chair for Bio-Medical Electronics, Ismaningerstr. 22, 81675 Munich, Germany
[d] Steinbeis-Transferzentrum Medizinische Elektronik und Lab on Chip-Systeme, Fendstr. 7, 80802 Munich, Germany

ARTICLE INFO

Keywords:
Impedance measurement
Fluorescence measurement
Dissolved oxygen measurement
AD5933
Live cell monitoring

ABSTRACT

Cell culture assays for therapeutic drug screening today are fully automated. Vitality of the cells is monitored by different sensors. For such a system, we propose a new reader unit, which is capable of reading two different fluorescent sensors and electrical impedance in 24-well-plates. Main goals are to reduce cost, complexity and size while achieving a similar performance as the existing reader unit. To achieve this, measurement electronics and signal paths for frequency domain fluorescence and bio-impedance measurement are combined. Central component is an integrated circuit for impedance spectroscopy. A new compact and economic optical setup is developed to read two different sensor spots on the bottom of the well. Measurement errors introduced by different components like DFT leakage, and frequency dependent signal delays are evaluated and compensated. A set of commercially available fluorescence sensor spots is used to verify the read out performance. The results are usable, with noise slightly higher than commercial readers. To verify the impedance measurement accuracy, measurements of known resistances are conducted. In the relevant impedance and frequency range for biological applications a suitable accuracy is achieved. Due to the higher sampling rate of the new reader, the higher noise can be reduced through averaging. The new system is significantly smaller and cheaper to manufacture than commercially available devices.

1. Introduction

Fluorescent probes for dissolved oxygen and pH are widely used in medical and environmental applications (Kohls et al., 1997; Shamsipur et al., 2008; Bagshaw et al., 2011; PreSens Precision Sensing GmbH, 2018). For example, such probes are needed for in-vitro cell monitoring (Wolf et al., 2013; Wolf et al., 1998; Seahorse Bioscience, 2018). For this application measuring and combining multiple parameters improves the reliability of the test results. The fluorescent sensor spots can be less than 2 mm in diameter, small enough to fit in a well of a 24 well plate. In addition to pH and pO2 sensors for metabolism rate measurements, impedance measurement is another key parameter for assessing cell physiology.

A combination of all three parameters is recorded in a recently developed device using a custom-designed 24 well plates, the intelligent microplate reader (IMR) (Wolf et al., 2013; Schwarzenberger et al., 2011). The special multi-well-plate was tested with cell-cultures for medicament screening. It has a special glass bottom with inter-digitated electrode structures for bio-impedance and two fluorescent sensor spots in each well. One for pH and one for pO2.

The physical principle of the dissolved oxygen measurement is based on fluorescence quenching by oxygen resulting in a decreased intensity and fluorescence lifetime. This is described by the Stern-Volmer equation:

$$\frac{I_0}{I} = 1+K_{sv}pO_2 = \frac{\tau_0}{\tau}.$$

Here, I is the intensity, τ the lifetime, K_{sv} a dye dependent constant and pO_2 the oxygen concentration. Values with index 0 indicate reference values for $pO_2 = 0$. Intensity measurement is often difficult due to error sources like impurities in the optical path, dirt, varying amounts of the dye or photo bleaching. Therefore, a lifetime based

* Corresponding author.
E-mail addresses: markus.hefele@tum.de (M. Hefele), walter.wirths@tum.de (W. Wirths), brischwein@tum.de (M. Brischwein), grothe@tum.de (H. Grothe), franz.kreupl@tum.de (F. Kreupl), wolf@tum.de (B. Wolf).

https://doi.org/10.1016/j.bios.2018.09.053
Received 29 June 2018; Received in revised form 3 September 2018; Accepted 13 September 2018
Available online 13 September 2018
0956-5663/

measurement is preferred. This can be done in the time domain by measuring the decaying emission after a short excitation pulse. The decay is exponential, such that with at least two sample points it is possible to calculate the lifetime. With this approach only the relative intensity change over a very short time period has to be evaluated and errors arising from the above-mentioned factors are therefore not substantial. Another method is to measure the lifetime in frequency domain. The fluorophore is exited with sinusoidal amplitude modulated light, resulting in an amplitude modulation in emission. Through the phosphorescent properties of the dye the emission is phase shifted with respect to the excitation by φ depending on the lifetime τ and modulation frequency f: $\tan\varphi = 2\pi\tau f$ (Wang and Wolfbeis, 2014).

Therefore, the detection is possible with a lock-in-amplifier which ensures high noise tolerance. On the electrical side measurement consists of the synthesis of a sinusoidal signal and detection of the system response in phase and amplitude. This is remarkably similar to complex impedance measurement, hence the same circuit can be applied. Optical pH-sensors use the so called dual-lifetime reference (DLR) to transform the intensity signal to a phase signal (Klimant et al., 2001), so the same measurement setup as for oxygen sensor spots is applicable.

In this work a simplified readout unit for the optical and electrical sensors for the IMR-multi-well-plates is presented to replace the complex and expensive former unit. The former optical unit consisted of two commercial fluorescence plate readers, each capable of reading 24 spots on a multi-well plate. With a complex and large setup of 96 optical fibers they were able to read 48 spots on the same size area. Impedance was measured with a separate, self-developed measurement unit (Schwarzenberger et al., 2011). The new unit shall combine the two measurement methods, provide a common data interface to a PC and reduce the height and price significantly.

2. Material and methods

The new measurement system is based on the Analog Devices AD5933 integrated network analyzer circuit. Two different analog frontends for impedance and fluorescence measurement are switchable with a multiplexer (MUX). A microcontroller is used for data processing. Fig. 1 shows a block diagram of the system.

2.1. Microcontroller (MCU)

An Atmel (now part of Microchip) ATmega328 (Microchip Technology Inc., 2018) integrated circuit is used to control the measurement device. It operates the multiplexers and controls the network analyzer and synthesizer. All data post-processing as described below is implemented in the firmware to be more independent on the host computer software and OS. The microcontroller accepts instructions from the host computer via serial interface (UART) either direct or via USB-serial converter. A human operable interactive and a computer command mode are available. All measurement data is sent back to the host computer in human readable form.

2.2. Network analyzer (NWA) AD5933

The AD5933 integrated circuit (Analog Devices, 2013) provides a complete impedance spectrometer backend for frequencies up to 100 kHz. It consists of a direct digital synthesizer (DDS) for excitation generation, preamplifiers, an analog to digital converter (ADC) and a single point discrete Fourier-transform (DFT) detector. All functions are controllable and data are transferred via I2C-bus.

However the AD5933 generates incorrect results under certain conditions caused by the discrete Fourier transformation, so called spectral leakage. Due to the transformation of a non-periodic sample, spectral energy seems to "leak" to adjacent frequency bins. These errors along with the appropriate troubleshooting measures have been described previously (Chabowski et al., 2015; Analog Devices, 2007a, 2007b; Stadnyk and Khoma, 2013). It is suggested to adjust the external system clock so that the sampled waveform becomes periodic to reduce the errors. However these adjustments are often realized by a variable divider and a fixed oscillator. An arbitrary clock frequency is therefore not possible, only integer factors. But the nature of the issue suggests, a fully tunable clock would be the best. Therefore a variable clock generator for the AD5933 is used.

2.3. Clock source AD9834 for AD5933

The AD9834 (Analog Devices, 2014) is a DDS integrated circuit. It itself needs an external reference clock, which is realized as a 50 MHz quartz oscillator. In this configuration the output frequency can be changed in steps of 0.19 Hz. It can produce a sinus or triangle signal. To produce a square signal as needed for the AD5933, the DDS is programmed to output a sine-wave. To smoothen the signal a RC-low-pass filter with a 3 dB bandwidth of 16.9 MHz is used. An external fast comparator ADCMP600 is connected to the differential output to generate a square-wave. The DDS is controlled by the microcontroller via a serial interface (SPI).

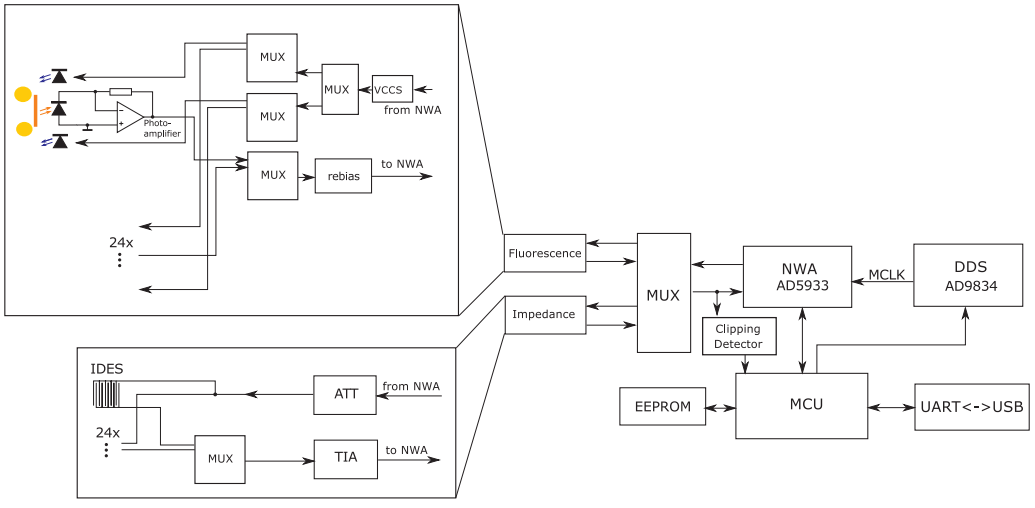

Fig. 1. Block diagram of the measurement system based on the AD5933 network analyzer (NWA). The blocks "Impedance" and "Fluorescence" are depicted in detail on the left side. A multiplexer (MUX) is used to switch between them. A direct digital synthesizer (DDS) is used for clocking. The whole system is managed by a microcontroller (MCU). The fluorescence block consists of a voltage controlled current source (VCCS) which is used to drive the LEDs and several multiplexers to switch through all LEDs and photodiodes. Every photodiode has a dedicated amplifier. The rebias circuit conditions the signal for the NWA. The impedance block contains an attenuator (ATT), a multiplexer and a transimpedance amplifier (TIA) to measure the current through the interdigitated electrode structures (IDES).

2.4. Impedance frontend

An attenuator (ATT) is needed to reduce the excitation signal to the desired level in the linear range of the electrode's characteristic line (Schwarzenberger et al., 2011). Higher amplitudes would push the electrochemical to nonlinear behavior and biological side effects could no longer be excluded. The DC bias of the signal is also transferred to Vcc/2. Afterwards the resulting current is amplified by a transimpedance amplifier (TIA) with an input level of Vcc/2 (see Fig. 1). This way there is no DC current flowing through the sensor electrodes which would cause unwanted electrode charging and Faraday currents. The amplifier's feedback resistor is switchable through an analog multiplexer for a wider measurement range. The appropriate range is selected by the microcontroller in dependence of the measured impedance values. An independent unit is used to detect clipping of the signal (see Fig. 1), as this would cause erroneous results.

2.5. Fluorescence sensor frontend

The fluorescent spots are excited by blue LEDs (Würth Elektronik, 150060BS75000, 470 nm) driven by a voltage controlled current source (VCCS) consisting of an operational amplifier and a MOSFET. The AD5933 produces a voltage signal, whereas the intensity of LEDs is determined by the current, hence the current source is required. The voltage signal has a DC bias which is higher than the amplitude, such that the current through the LED never turns zero. This is in contrast to the impedance frontend, where the DC bias has to be zero. Analog multiplexers are used to connect the source to all 48 LEDs (see Fig. 1). During stand-by the current source is connected to a dummy load, so that all LEDs are dark and the fluorophore is not degraded further.

The fluorescence light is detected by photodiodes (VISHAY, VBPW34S). A long-pass color filter is used to block the excitation light. The photodiode current is amplified by a trans-impedance amplifier OPA380 with a 1 MOhm feedback resistor. The signal is then re-biased to a DC-level of Vcc/2 for the AD5933.

To place all components for the optical interface on an area of a standard 24-well plate, only one photodiode per well is employed. It is used to detect light from two sensor spots. To excite only one spot at a time, a single dedicated LED is used for every of the in total 48 spots. The LEDs have a size of $1.6 \times 0.8\,mm^2$, whereas the photo-detectors are $4.4 \times 3.9\,mm^2$ to catch as much light as possible. All other components are placed on the back of the printed circuit board (PCB), so that a laser-cut opaque acrylic mask can be placed on top of the board (see Fig. 2a). The mask prevents the excitation of adjacent spots and acts as a spacer to keep a defined distance. The emission filter is a coated film from Rosco Laboratories Inc. (Stamford, CT), e-color+ "deep orange" #158, with a low-pass characteristic and a cutoff wavelength of 550 nm. For easier assembly holes for the excitation light are laser cut and the whole sheet is glued between the two parts of the mask like a sandwich. A cross section of the optical setup is shown in Fig. 2b. The total height of the optics from the lower side of the PCB to the top of the mask is 5 mm. With the components on the backside and connectors the total height of the device is below 1 cm.

2.6. Test objects

To test the accuracy of the impedance measurement several resistors are used, as well as a RC-network consisting of a 1 kOhm resistor in series with a parallel circuit of a 2 kOhm resistor and a 30 nF capacitor. Impedance measurements were validated with a Solartron 1260 Impedance analyzer (0.1%, 0.1° accuracy).

Fluorescence measurements were tested with PreSens Precision Sensing GmbH, 2018 oxygen and pH sensor-spots and fluorescein. Fluorescein has a fluorescence lifetime of 4 ns (Magde et al., 1999) and therefore causes nearly no phase-shift in the measurement range up to 100 kHz.

2.7. Error correction and spectral leakage prevention

To prevent spectral leakage the external clock is adopted to the desired measurement frequency $f_{measure}$. The clock frequency f_{CLK} is determined by $f_{measure}/m*2^{14}$, whereas m is an arbitrary integer. m was chosen to be 100 to ensure the maximum clock frequency does not exceed the limit of 16.7 MHz of the AD5933 at 100 kHz measurement frequency. But even this resulted in a phase shift depending on measurement frequency. Therefore this shift was measured and fitted to a function. With this function it is possible to eliminate the errors. As the shift depends also on m, the integer m was set to a fixed value to simplify the corrective function.

Error correction is achieved in several steps. First the errors of the AD5933 were characterized and compensated. This was done for the impedance as well as for the fluorescence analog frontend. To measure only the AD5933 without any disturbance through the frontends a multiplexer is used to directly loopback its output to the input. This multiplexer also switches between impedance and fluorescence measurement. The phase error of the AD5933 was found to be non-linear with frequency, therefore a piecewise function is used for modeling. It consists of an exponential function followed by two linear functions. Their parameters were fitted to the measured error. A similar procedure was used for the errors in amplitude, but only a linear function was necessary. These errors occur presumably due to the implementation of the DFT and delayed sampling at higher frequencies (Chabowski et al., 2015).

The impedance frontend has a multiplexer which connects the 24 electrode pairs and also some test resistors for calibration. The later are used to calibrate the interface. The adjustment is achieved with affine linear functions for each feedback resistor of the trans-impedance amplifier. They are calculated automatically by the firmware of the microcontroller.

The optical frontend also expresses a phase error. Due to the complicated error function a look-up-table is utilized and stored in the EEPROM. Interim values are linearly interpolated. The generation of this table is described in Section 3.2.

3. Results

To verify the performance of the reader unit, several experiments were conducted for impedance and fluorescence lifetime measurement.

3.1. Impedance measurement

Several resistors were measured at frequencies from 1 kHz to 100 kHz. It was observed that low resistances resulted in a phase and amplitude error at high frequencies.

At 99.5 kHz the error for resistance of 124 Ω was at a maximum of 49%. For 99.5 kHz the error was below 1% for resistances below 10 kOhm. This effect is caused by the impedance frontend. To test the performance for frequency dependent impedances a RC-network was comparatively measured with the solartron instrument and the IC device. The network was also simulated in SPICE (see Fig. 3). Good results are obtained for a medium frequency range with relative amplitude errors from − 2% to 2%. For low and high frequencies the accuracy of the AD5933 is not as good as the Solartron. Maximum relative amplitude error was observed 3% at 2 kHz. Maximum absolute phase error was 8.5° at 100 kHz.

As an electrochemical system, an inter-digitated electrode structure immersed in phosphate buffered saline was measured and compared to the Solartron (see Fig. 4). The results are similar, only for high frequencies the phase differs. The small step at ca. 4 kHz in the AD5933 graph is caused by the auto range functionality of the impedance frontend.

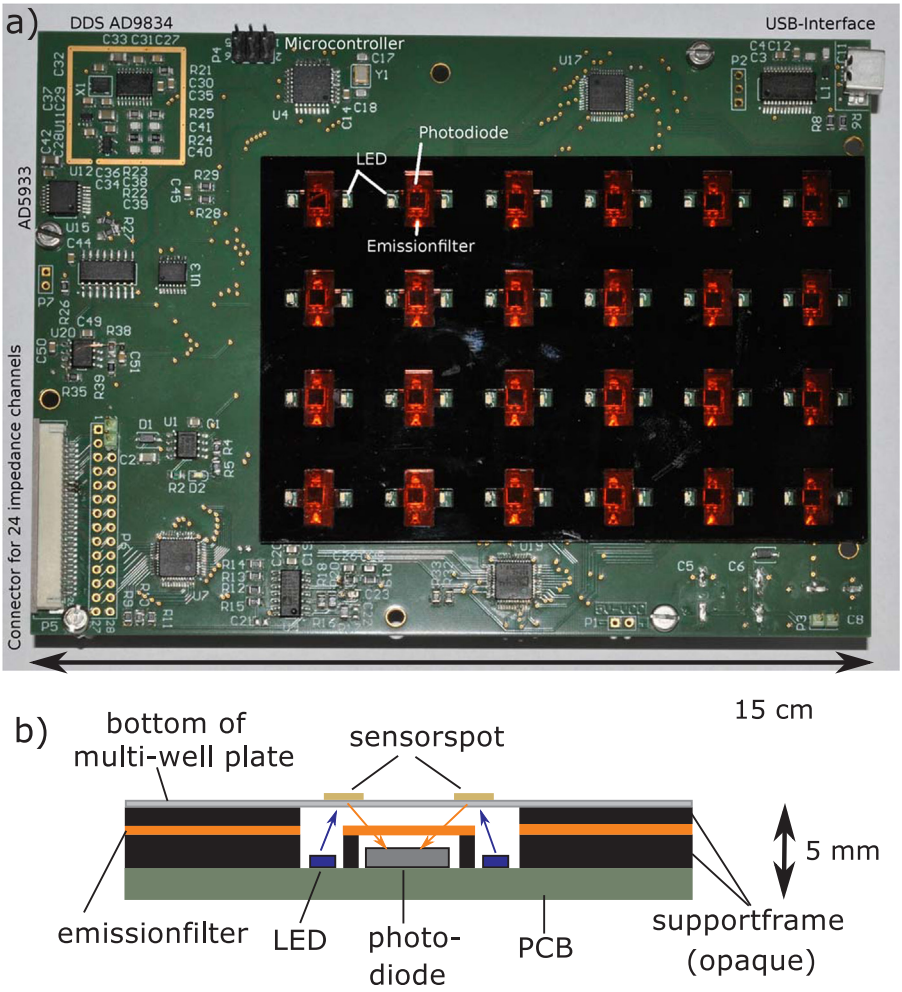

Fig. 2. a) Photograph of the PCB with optical setup in place. b) cross section of the optics. It consists of several layers with unique laser-cut holes. A blue LED (470 nm) is used to excite the fluorescent sensor spot. The emission light is then filtered through a matched filter foil before it hits the photodiode. One photodiode can read two spots sequentially to save space.

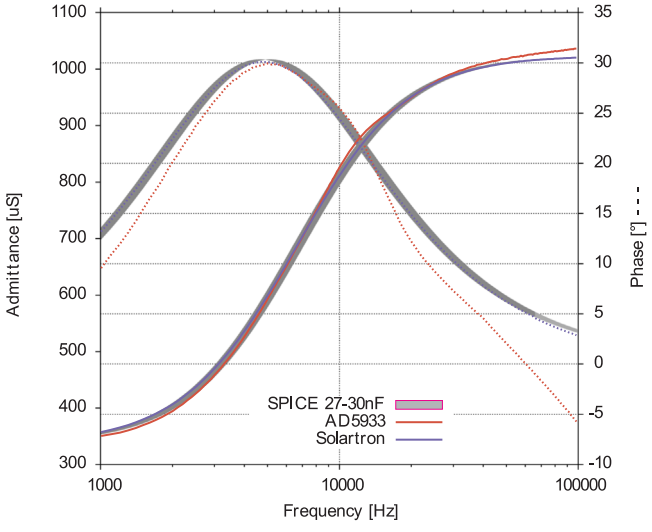

Fig. 3. Comparison of the developed impedance spectrometer to a Solartron 1260 impedance analyzer measuring a RC-Network. The amplitude is drawn in solid line, the phase value is dotted. The Network was also simulated with SPICE. Due to limited measurement accuracy for the capacitor a range from 27 nF to 30 nF was simulated.

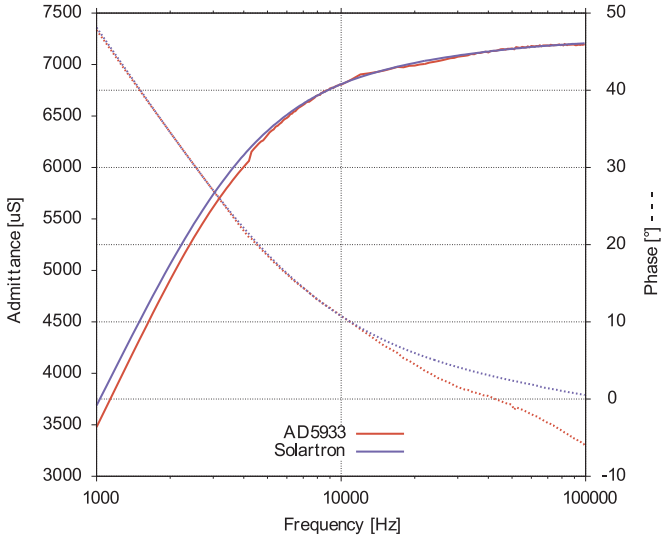

Fig. 4. Comparison of the developed impedance spectrometer to a Solartron 1260 impedance analyzer measuring an inter-digitated electrode structure (IDES) submerged in phosphate buffered saline (PBS). The amplitude is drawn in solid line, the phase value is dotted.

3.2. Fluorescence measurement

The first measurements were conducted with fluorescent plastic plates and fluorescein solved in alkaline water. These materials should not show a phase shift at the measured frequencies due to their very short fluorescence lifetime. The measured phase shift is caused by the system. This measurement was used to create the look-up-table for phase correction.

To evaluate the noise of the measurement system, an oxygen sensor spot was measured in air every second for an hour at a modulation frequency of 40 kHz. Each measurement illuminates the spot for about 6 ms. The phase noise was normally distributed with a medium value of − 46.83° and standard deviation of 0.274°. For a fluorescent plastic plate the standard deviation was 0.198°. The amplitude noise showed no normal distribution, indicating other than random sources of the deviation. Cross-talk between spots of a shared photodiode could not be observed.

Finally, to verify the functionality of the fluorescence interface with the target dyes, two experiments were conducted:

3.2.1. Oxygen probe performance

A well of a multi-well plate equipped with oxygen sensor spots (PreSens GmbH, Germany) was filled with distilled water with oxygen saturation (relative to air) of 100%, 50% and 0% subsequently. In-between the well was emptied. Phase was measured with a sampling frequency of 2.5 Hz at a modulation frequency of 40 kHz. The signal was noisy with a standard deviation of 0.22°, but the different concentration levels are clearly distinguishable (Fig. 5). The change from 100% to zero resulted in a total 5° phase shift. This translates to 0.05° per 1% point oxygen saturation, and thus a standard deviation of 4.4% points oxygen saturation. For concentrations lower than 100% the slow re-diffusion of oxygen from the ambient air can be observed because the well was not sealed. Also a change in fluorescence amplitude occurs. While the well was empty, amplitude was significantly higher and phase dropped to levels similar to water with 0% oxygen. At very low concentrations, the measurement signal seemed not to be stable. This could be caused by residues of water from the previous sample with higher oxygen levels, which mix slowly with the new sample, thus the sensor sees varying concentrations.

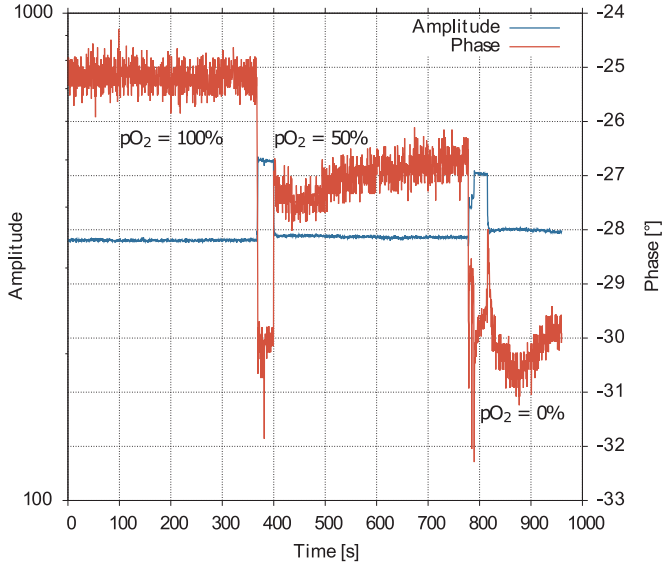

Fig. 5. Measurement of fluorescent oxygen sensor spots with three different water samples with oxygen saturation relative to air of 100%, 50% and 0% at a single frequency of 40 kHz over time. The amplitude stays constant whereas the phase of the modulated light changes with oxygen saturation. When the vessel is emptied for the new sample, the amplitude rises. During this time phase measurements are unreliable. For concentrations lower than 100% air saturation, a re-diffusion of oxygen is observed due to the open vessel. Due to inhomogeneous oxygen distribution caused by residues and the following equilibration a small drop of the phase can be observed from t = 810 s till 870 s.

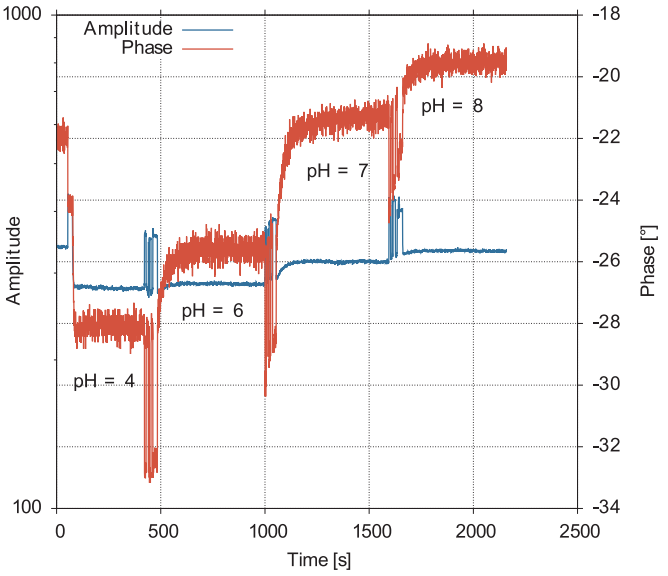

Fig. 6. Measurement of fluorescent pH sensor spots with four pH buffers at a single frequency of 40 kHz over time. The phase of the modulated light changes with pH. Here also the amplitude is slightly dependent on the change. The relation between pH and phase is non-linear. During buffer exchange, the measurement is unreliable.

3.2.2. pH probe performance

The readout of the pH sensor (PreSens GmbH, Germany) was tested in a similar way. Four different pH-buffers (Merck Titrisol) ranging from pH = 4 to pH = 8 were filled in a well with distilled water flushing in-between. The results are plotted in Fig. 6. The phase to pH relation is non-linear, with the highest sensitivity at pH = 6–7. With a standard deviation of 0.23° at pH = 7 and a maximum of 4.3° per pH-step at around pH = 6.5, this results in a standard deviation of 0.054 pH-steps of the measurement. For lower and higher pH-ranges this precision is worse as the same phase noise will result in a larger pH-noise due to lower sensitivity of the dye.

4. Discussion

Using a common backend for impedance and fluorescence measurement is feasible, simplifies the circuit design and efficiently uses resources. Redundant structures can be removed and combined for better performance and easier maintenance. The new assay measurement device is consistent in control and data format. Different measurement devices for pH, pO_2 and impedance from different manufacturers with usually different and non-compatible interfaces are no longer required. This concept is not limited to the use of the AD5933. It could be replaced by a similar one (e.g. the ADUCM350) or any other network analyzer circuit.

The new concept for the optical setup decreases the size significantly from 18 cm height of the old fiber optic unit to about 1 cm (without case). Therefore a standard pipetting robot can now be used for cell assays. A custom designed, and therefore expensive robot as used for the IMR is no longer necessary. All parts of the reader can be produced with standard machine processes such as PCB assembly and laser cutting. Compared to setups with fiber optics like in the old version of the IMR, this results in much lower production cost. Also contributing to cost reduction is the reduction of the photodiodes without introducing cross-talk between sensor spots of a shared diode. All those

improvements did not cause negative side effects regarding measurement performance.

Using a variable external clock for the AD5933 as mentioned in the manufacturers application note combined with the additional steps described in Section 2.7 was found being the most simple and effective method to reduce errors caused by spectral leakage. Due to the high cost for the DDS circuit, nearly as expensive as the AD5933, this solution is not the cheapest. But it provides full flexibility in measuring throughout the whole frequency range accurately.

Fluorescence measurement raw data is noisier than for commercially available readers, but the SNR can be improved by averaging multiple data points as the noise is normally distributed. One measurement takes approximately 6 ms. Therefore, nine or more measurements can be obtained without even getting close to the time constants of the typical pH or pO2 change, reducing the noise by factor 3 or more. Thus it reaches a similar precision as the PreSens SDR Reader, which is rated as ± 0.1 pH at pH = 7 (PreSens Precision Sensing GmbH, 2018). The developed reader shows at the same pH a standard deviation of 0.054 pH without averaging, hence 99% of the data points are within a window of ± 0.15 pH. By averaging, this can be further reduced. For pO2 measurement this figure is slightly worse, hence more averaging is required.

This shows, that the fluorescence reader reaches a similar performance as comparable commercial devices. The main limitations of this sensor-system are now the dyes, which by itself exhibit different error sources like aging, cross-sensitivity, hysteresis, etc. (Kohls et al.,1997; Shamsipur et al., 2008).

The impedance measurement showed significant errors in phase measurement for frequencies above 20 kHz or impedances below 1 kOhm. This was mainly caused by the operational amplifiers of the analog frontend. It could be improved further by reworking the analog frontend, i.e., by using a faster operational amplifier. For frequencies around 10 kHz, as used for bio-impedance measurements, the current design is still suitable and has a similar performance as the IMR (Wolf et al., 2013; Schwarzenberger et al., 2011).

5. Conclusion

We demonstrated a new combined reader unit for label free cell assays in mult-well-plates carrying fluorescence sensor spots for pH and pO2 and impedance sensing electrode structures which drastically reduces size and cost. This approach was possible by using a common signal processing backend for these two different sensor types. Redesigning the optic assembly resulted in a less complex and therefore cheaper setup. The demonstrated sensitivity of the reader is suitable for its designated task to replace an existing reader unit in the cell assay system.

Despite the achieved size reduction compared to previous bulky readers, further design iterations such as the use of two stacked PCBs will allow to reduce the total footprint area to that of a standard multi-well-plate. With a different, more carefully designed impedance analog frontend, impedance measurement range and accuracy could be further increased. By replacing the AD5933 subsystem through either a more economic or a more powerful digital signal processor (DSP) with integrated analog and digital converters, cost or accuracy can be optimized according to the requirements for the desired application.

In future this new device will undergo tests in cellular-assay systems for therapeutic drug screening.

Acknowledgement

The Authors thank the “Heinz Nixdorf-Stiftung” for its support.

Declarations of interest

None

References

Analog Devices, 2007. Application Note 843 Measuring a Loudspeaker Impedance Profile Using the AD5933.
Analog Devices, 2007. Evaluation Board for the 250 kSPS 12-Bit Impedance Converter Network Analyzer.
Analog Devices, 2013. AD5933 1 MSPS, 12-Bit Impedance Converter, Network Analyzer.
Analog Devices, 2014. AD9834 20 mW Power, 2.3 V to 5.5 V, 75 MHz Complete DDS.
Bagshaw, E.A., Wadham, L.J., Mowlem, M., Tranter, M., Eveness, J., Fountain, A.G., Telling, J., 2011. Determination of dissolved oxygen in the cryosphere: a comprehensive laboratory and field evaluation of fiber optic sensors. Environ. Sci. Technol. 45 (2), 700–705. https://doi.org/10.1021/es102571j.
Chabowski, K., Piasecki, T., Dzierka, A., Nitsch, K., 2015. Simple wide frequency range impedance meter based on AD5933 integrated circuit. Metrol. Meas. Syst. 22, 13–24.
Klimant, I., Huber, C., Liebsch, G., Neurauter, G., Stangelmayer, A., Wolfbeis, O., 2001. Dual lifetime referencing (DLR) — a new scheme for converting fluorescence intensity into a frequency-domain or time-domain information. In: Valeur, B., Brochon, J.C. (Eds.), New Trends in FluorescenceSpectroscopy 1. Springer Berlin Heidelberg, pp. 257–274 (Springer Series on Fluorescence).
Kohls, O., Klimant, I., Holst, G.A., Kuehl, M., 1997. Development and comparison of pH microoptodes for use in marine systems. Micro- Nanofabricated Electro-Opt. Mech. Syst. Biomed. Environ. Appl. Int. Soc. Opt. Photonics 82–92 (S.).
Magde, D., Rojas, G.E., Seybold, P.G., 1999. Solvent dependence of the fluorescence lifetimes of xanthene dyes. Photochem. Photobiol. 70, 737–744.
Microchip Technology Inc., 2018. ATmega328 ⟨https://www.microchip.com/wwwproducts/en/ATmega328⟩ (Accessed 27 July 2018).
PreSens Precision Sensing GmbH, 2018. ⟨http://www.presens.de/products/brochures/category/systems/brochure/sdr-sensordish-reader.html⟩ (Accessed 21 June 2018).
Schwarzenberger, T., Wolf, P., Brischwein, M., Kleinhans, R., Demmel, F., Lechner, A., Becker, B., Wolf, B., 2011. Impedance sensor technology for cell-based assays in the framework of a high-content screening system. Physiol. Meas. 32, 977.
Seahorse Bioscience. 2018. ⟨https://www.agilent.com/en/products/cell-analysis/seahorse-analyzers⟩ (Accessed 21 June 2018).
Shamsipur, M., Abbasitabar, F., Zare-Shahabadi, V., Shahabadi, Akhond, M., 2008. Broad-range optical pH sensor based on binary mixed-indicator doped sol-gel film and application of artificial neural network. Anal. Lett. 41. Jg. (Nr. 17), 3113–3123 (S.).
Stadnyk, B., Khoma, Y., 2013. Improving the accuracy of the single chip impedance analyzer for sensor applications. Sens. Transducers 150, 27.
Wang, Xd, Wolfbeis, O.S., 2014. Optical methods for sensing and imaging oxygen: materials, spectroscopies and applications. Chem. Soc. Rev. 43, 3666–3761.
Wolf, B., Kraus, M., Brischwein, M., Ehret, R., Baumann, W., Lehmann, M., 1998. Biofunctional hybrid structures—cell–silicon hybrids for applications in biomedicine and bioinformatics. Bioelectrochemistry Bioenerg. 46, 215–225.
Wolf, P., Brischwein, M., Kleinhans, R., Demmel, F., Schwarzenberger, T., Pfister, C., Wolf, B., 2013. Automated platform for sensor-based monitoring and controlled assays of living cells and tissues. Biosens. Bioelectron. 50, 111–117.